

Please cite the Published Version

Pytlak, Anna, Sparkes, Robert, Goraj, Weronika, Szafranek-Nakonieczna, Anna, Banach, Artur, Akmetkaliyeva, Saule and Słowakiewicz, Mirosław (2021) Methanotroph-derived bacteriohopanepolyol signatures in sediments covering Miocene brown coal deposits. *International Journal of Coal Geology*, 242. p. 103759. ISSN 0166-5162

DOI: <https://doi.org/10.1016/j.coal.2021.103759>

Publisher: Elsevier BV

Version: Accepted Version

Downloaded from: <https://e-space.mmu.ac.uk/627718/>

Usage rights:  [Creative Commons: Attribution-Noncommercial-No Derivative Works 4.0](https://creativecommons.org/licenses/by-nc-nd/4.0/)

Additional Information: This is an Author Accepted Manuscript of an article published in *International Journal of Coal Geology*.

Enquiries:

If you have questions about this document, contact openresearch@mmu.ac.uk. Please include the URL of the record in e-space. If you believe that your, or a third party's rights have been compromised through this document please see our Take Down policy (available from <https://www.mmu.ac.uk/library/using-the-library/policies-and-guidelines>)

1 **METHANOTROPH-DERIVED BACTERIOHOPANEPOLYOL SIGNATURES IN**
2 **SEDIMENTS COVERING MIOCENE BROWN COAL DEPOSITS**

3 **Anna Pytlak**¹, **Robert Sparkes**², **Weronika Goraj**³, **Anna Szafranek-Nakoneczna**³, **Artur**
4 **Banach**³, **Saule Akmetkaliyeva**² **Mirosław Słowakiewicz**^{4,5}

5 1. *Institute of Agrophysics, Polish Academy of Sciences, Doświadczalna 4, 20-290 Lublin, Poland*

6 2. *Ecology and Environment Research Centre, Department of Natural Sciences, Manchester*
7 *Metropolitan University, Oxford Road, Manchester M15 6BH, UK*

8 3. *Institute of Biological Sciences, The John Paul II Catholic University of Lublin, Konstantynów 1i,*
9 *20-708 Lublin, Poland*

10 4. *Faculty of Geology, University of Warsaw, Żwirki i Wigury 93, 02-089 Warszawa, Poland*

11 5. *Kazan Federal University, Kremlovskaya 18, 420008 Kazan, Russia*

12

13 **Highlights**

14 Methanotroph-specific BHPs were more abundant in lignites than in mineral samples.

15 The significant role of intrinsic methane turnover in lignites is suggested.

16 Content and speciation of BHPs depend on the diagenetic conditions.

17 High diagenetic temperature is suggested to cause aminopentol and 3-Me BHT breakage.

18 The intrinsic methane turnover may have an influence on biogas-production potential.

19

20 **Abstract**

21 Methanotrophic bacteria (MB) are an important group of microorganisms, involved in the
22 greenhouse gas (GHG) cycles. They are responsible for the utilization of methane, one of the main
23 GHGs, which is released in large amounts (*via* biogenic and abiogenic processes) during coal
24 formation. This study aimed to determine the main factors affecting the distribution of the MB in
25 two lignite-bearing series of the Turów and Bełchatów coal basins. Distribution of MB in the lignite
26 profiles was studied using methanotroph-specific lipid biomarkers such as amino-
27 bacteriohopanepolyols (NH-BHPs) and C-3 methylated BHPs. BHP results were combined with

28 physical and chemical properties of the studied sediments. In general, lignites were richer in BHPs
29 than the mineral samples, which points to the important role of the intrinsic methane cycling. NH-
30 BHP speciation confirmed that the methanotrophic community of the studied sediments was a
31 combination of both type I and, especially, type II methanotrophs. Based on geological data, it was
32 suggested that elevated temperature during diagenesis intensifies decomposition of methanotroph-
33 specific biomarkers (aminopentol and 3-Me BHT). It was found that the tested BHPs can derive
34 from both fossil and living MB. The presence of metabolically active methanotrophs should
35 therefore be accounted for during studies aimed at using lignite deposits as a source of methane.

36

37 *Keywords: Biomarkers; Methanotrophy; Bacteriohopanepolyols; Methane; Lignite; Miocene*

38 **1. Introduction**

39 Disturbances in homeostasis of the global environment are one of the most important present-
40 day concerns. There is no doubt that the planet is warming, and the climate changing. For this reason,
41 questions about the transformation of greenhouse gases (GHG) in the environment, although raised for
42 decades, have not lost their significance.

43 Amongst the GHG, methane is one of the most important (Edenhofer et al., 2015; Walkiewicz
44 et al., 2020). The origin of much of the atmospheric methane is attributed to the fossil fuel deposits (i.e.
45 hard coal and lignite seams) (Barkley et al., 2019). It was already shown that within an undisturbed
46 geological systems, methane emissions may be notably balanced by microbial methanotrophic activity
47 (Pytlak et al., 2014; Stepniewska et al., 2014; Thielemann et al., 2000). Human activity, leading to
48 disruption of the protective sheath of coal overburden, is therefore responsible for the vast majority of
49 the methane exchange between the underground deposits and the atmosphere (Kholod et al., 2020).

50 Numerous studies have shown the environmental importance of aerobic methanotrophic
51 bacteria (MB) which are able to attenuate net CH₄ fluxes with high efficiency and play an important
52 role in shaping the global GHG balance (Dean et al., 2018; Pandey et al., 2014). . Those which were
53 dedicated to various aquatic and terrestrial environmental niches described natural succession of the

54 microbial communities, manifested by an increased number of methanotrophic bacteria or enhanced
55 methanotrophic activity in response to the increased supply of methane (Mayr et al., 2020; Walkiewicz
56 et al., 2012; Włodarczyk et al., 2004).

57 Investigations concerning the present-day methanotrophic communities rely on DNA- or
58 RNA-based approaches which provide a precise picture of bacterial abundance and activity (Chiri et
59 al., 2020; Pandit et al., 2018). These tools, however, have limited application to reconstructions of
60 microbial processes in longer timeframes. Most of the nucleic acids released into the environment are
61 rapidly degraded under the influence of biotic and abiotic factors. RNA degradation time is measured
62 in minutes. DNA is more stable (Marshall et al., 2021), under favourable conditions (e.g. association
63 with minerals, sand and humic acids) it can survive for long periods of time (Cai et al., 2006).
64 Numerous studies (summarized by (Arning and Wilson, 2020; Pedersen et al., 2015) evidenced
65 preservation of prokaryotic DNA in the sedimentary series dated thousands or even millions of years
66 back. The majority of these records were found in permafrost conditions; the oldest DNA records
67 come from the Antarctic ice cores and date back to 8 million years (Bidle et al., 2007). However, as
68 described by (Ellegaard et al., 2020), in sediments that are not permafrost and contain an active
69 microbial community, the ancient DNA is not only degraded, but also, with time, becomes
70 overwhelmed with the genetic material of modern microorganisms that are adapted to the current
71 environmental conditions, which poses a threat of palaeorecord disappearance.

72 On the other hand, lipid biomarkers are known for superior preservation over longer time
73 periods (Cappellini et al., 2018; Ellegaard et al., 2020), which by far exceed the preservation period
74 of DNA. It is documented, that in contrast to nucleic acids, high proportion of the lipid biomarkers
75 remain intact after cell death (Osborne et al., 2017). The pentacyclic ring of BHPs is highly resistant,
76 therefore the characteristic structures as well as their degradation products are preserved in the
77 geological record and found ubiquitously in fossils (Goryl et al., 2018; Kusch et al., 2021). The
78 accumulated BHPs thus comprise a record of the processes taking place in the studied environment
79 since deposition till nowadays. Occurrence of the fossilized BHPs was already used for reconstruction

80 of microbial processes in ancient sediments (up to several Ma old), e.g. sea bottom (Rush et al., 2019;
81 Talbot et al., 2014) and lignite (Talbot et al., 2016).

82 The cell membranes of MB contain an array of hopanoids including common (produced also by
83 other bacteria) diploptene and diplopterol as well as various extended hopanoids with multiple
84 functional groups. It was previously suggested that C-3 methylation and ¹³C depletion were possible
85 indicators of methanotrophic BHPs origin (Zundel and Rohmer, 1985). However, (Sinninghe Damsté et
86 al., 2017; Rush et al., 2016) revealed that *hpnR* gene encoding hopanoid C-3 methylase can also be
87 found in other microorganisms such as acetic acid bacteria. Furthermore, the presence of *hpnR* was
88 confirmed only in 3 out of 9 studied MB genomes (Welanders and Summons, 2012). There is also an
89 evidence that not all MB-derived hopanoids show a depleted carbon isotope signature. According to
90 (Jahnke et al., 1999) BHPs derived from type II methanotrophs may not only be less ¹³C depleted than
91 from type I but even enriched with respect to the CH₄ substrate. These observations were confirmed also
92 by studies of the type II-dominated natural ecosystems (Inglis et al., 2019) and are of particular
93 importance while considering distribution of methanotrophic bacteria in complex geological settings
94 where variable ecological niches and differences in major factors affecting competition between type I
95 and type II methanotrophs occur (Graham et al., 1993; Knief, 2015).

96 The most diagnostic BHPs for MB are thought to be aminobacteriohopanes (NH-BHPs) (Rush
97 et al., 2016), of which 35-aminobacteriohopane-30,31,32,33,34-pentol (aminopentol; [1d]) is
98 synthesized almost exclusively by the type I (*Gammaproteobacteria*) MB. The other NH-BHPs
99 produced by MB in large quantities are 35-aminobacteriohopane-31,32,33,34-tetrol (aminotetrol; [1c])
100 and 35-aminobacteriohopane-32,33,34-triol (aminotriol; [1b]), which are found in almost all type I and
101 type II (*Alphaproteobacteria*) MB (except for *Methylocella*). Aminotetrol is less source-specific because
102 it is also synthesized by sulfate reducing bacteria (SRB) of the genus *Desulfovibrio*. Aminotriol, which
103 is one of the main BHPs found in the type II and verrucomicrobial MB, is also produced by some other
104 aerobic bacteria (Sinninghe Damsté et al., 2017). Studies of bacterial cultures show that the probability
105 that aminotetrol is derived from the methanotrophs is linked to increase in the aminotetrol/aminotriol
106 ratio (with proportion lower than 1:20 suggesting non-methanotrophic origin) (Rush et al., 2016). BHP

107 structures are included in Supplementary Figure 1, and referred to in the manuscript within square
108 brackets).

109 Analysis of the NH-BHP seems the most reliable method to study occurrence and activity of the
110 methanotrophic bacteria in the geological record and because methanotrophy generally tracks methane
111 concentrations - also carbon cycling (Inglis et al., 2015; Pancost et al., 2007). In the present study, the
112 BHP (NH-BHPs and C-3 methylated BHPs) records, in combination with results concerning physical
113 and chemical properties, were used to determine the role of various lignite layers in limiting the methane
114 stream entering the atmosphere in two lignite series of the Turów and Bełchatów coal basins.

115 **2. Material and methods**

116 **2.1. Sampling site**

117 Bełchatów deposit (BD; central Poland) is located in the Kleszczów Graben, a longitudinal
118 tensional structure formed along pre-existing (Variscan) fault zones as a result of compensation
119 movements in the foreland of the Alpine folding zone (Myśkow et al., 2016). The graben is filled with
120 Paleogene and Neogene sediments underlain by Upper Jurassic limestones and Upper Cretaceous gaaizes.
121 Coal-bearing sediments associated with productive complex are considered to be an equivalent of the
122 3rd Ścinawa lignite seam (SLS-3) in the lower part, and 2nd Lusatian lignite seam (LLS-2) in the upper
123 part (Fig 2; (Pawelec and Bielowicz, 2016; Widera, 2016a). Lignite seams are covered with a series of
124 Tertiary and Quaternary sandy and clayey formations of fluvio-lacustrine origin. Sedimentation of the
125 lignite overburden was driven mainly by the autochthonic cyclic subsidence (related to the lignite
126 compaction). Quaternary deposits are thick (up to dozens of metres) and associated with glacial
127 processes (Mastej et al., 2015; Widera, 2016b).

128 Turów deposit (PGT) is a part of the Zittau Basin, which extends across Germany, Poland and
129 the Czech Republic. This extensive depression (15 km long and 7 km wide), similarly to the BD, is filled
130 with Miocene coal-bearing series. PGT lignites are of similar age to those found in the PGB (ŚLS-3 and
131 LLS-2). The overburden is built of clay, sand and gravel that are related to auto- and allochthonous
132 sedimentary cycles (Kasiński, 1983). Tertiary formations are covered by Quaternary sediments,

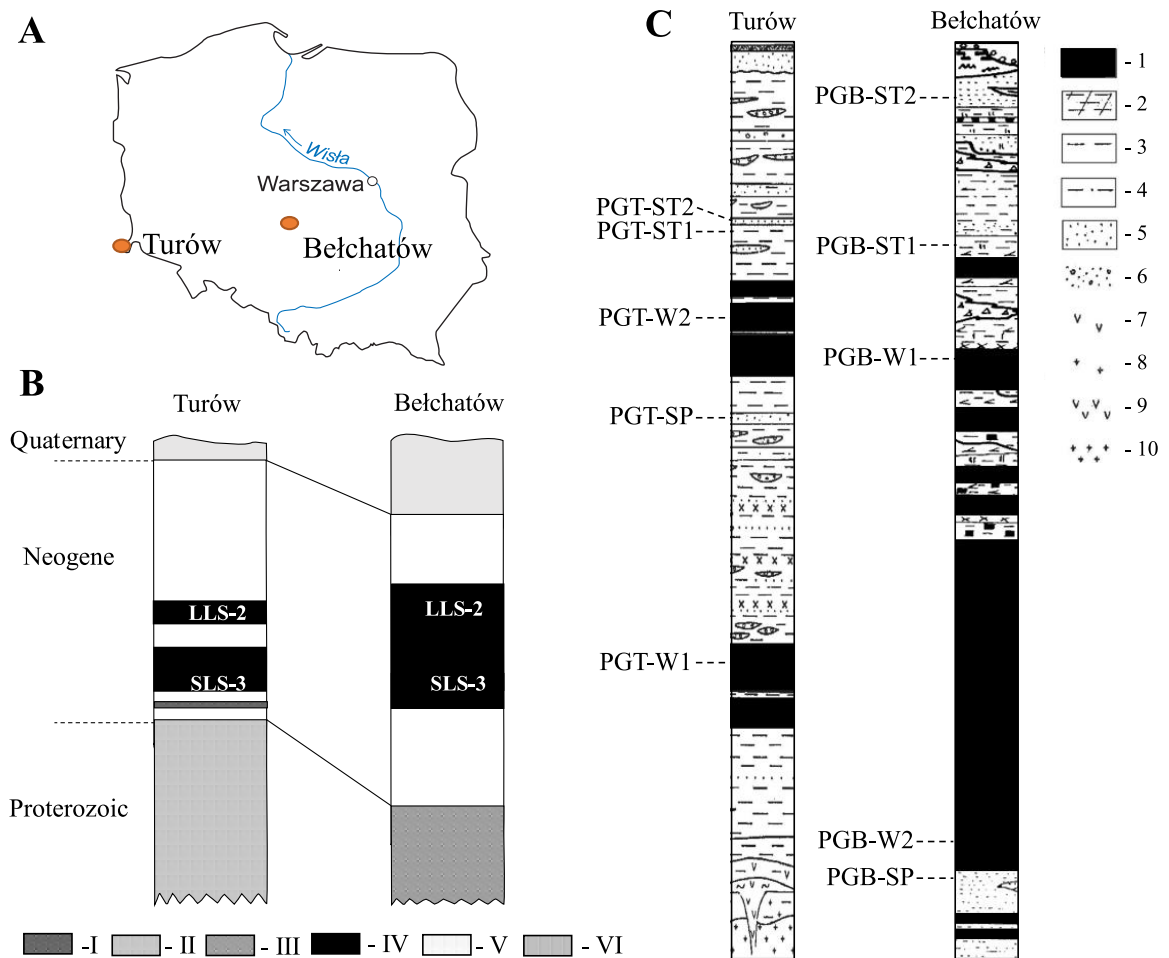
133 generally not exceeding several metres. Miocene brown-coal formation and Cenozoic clastic deposits
 134 are underlain by granitoids (Liber-Makowska, 2013).

135 Samples were obtained courtesy of the PGE GiEK S.A. from the opencast mines exploiting
 136 Bełchatów (51°15'46.4"N 19°18'49.2"E) (PGB) and Turów (50.9124°N 14.9031°E) (TD) deposits (Fig.
 137 1) (Table 1). In each object, materials were collected from temporary exposures, created by mining
 138 operations. Samples (4 – 5 kg each) were immediately put into sterile, hermetic plastic bags. Soon after
 139 transportation, subsamples were collected from the interior of the clumps using sterile and alcohol rinsed
 140 tools. A separate set of tools was used for each of the samples. The specimens aimed to be used for BHP
 141 analyses were kept frozen at -20 °C.

142 Tab. 1. Lithostratigraphic characteristics of samples.

Symbol	Location in the deposit	Lithology	Genetic processes	Depth m.b.s.*
Bełchatów				
PGB-ST2	clay-sand complex	gray sand	glaciolacustrine sed.	-48
PGB-ST1	clay-coal complex	gray-greenish sandy loam	fluvio-lacustrine sed.	-108
PGB-W1	coal complex	lignite	coal diagenesis	-112
PGB-W2	coal complex	lignite	coal diagenesis	-156
PGB-SP	sub-coal complex	dark gray-brown clay	lacustrine sed.	-158
Turów				
PGT-ST2	clay-sand complex	sand/gravel	fluvial sed. (cyclic)	-167
PGT-ST1	clay-sand complex	clay	fluvial sed. (cyclic)	-167
PGT-W2	coal complex	lignite	coal diagenesis	-170
PGT-SP	interbedded sandy complex	sandstone	fluvial sed.	-220
PGT-W1	coal complex	lignite	coal diagenesis	-255

143 *m.b.s. – metres below surface



144

145

146

147

148

149

150

Fig. 1. Location of sampling sites (A), lithology (B) and stratigraphic position (C) of the studied profiles. I – volcanoclastic, II – igneous rocks , III – limestone , IV – lignite, V – clayey and sandy formations , VI – Quaternary cover; 1 - lignite, 2 – coaly clay, 3 - clay, 4 - silt , 5 - sand , 6 – sand with gravel, 7 – weathered effusive rocks , 8 – weathered crystalline rocks, 9 – effusive rocks, 10 – crystalline rocks; SLS-3 – 3rd Ścinawa lignite seam, LLS-2- 2nd Lusatian lignite seam; modified after (Ratajczak and Hycnar, 2017; Widera, 2013).

151

2.2. Determination of physical and chemical properties

152

153

154

155

Prior to laboratory analysis, samples were crushed to $\varphi < 2$ mm. Moisture was determined gravimetrically by oven-drying to a constant weight at 105 °C, directly after collecting the samples. Reaction (pH) and electrolytic conductivity (EC) were determined after full saturation of the powdered sediments with water, using a multifunctional potential meter pIONneer 65 (Radiometer Analytical

156 S.A., France) equipped with a glass electrode (Cartrode pH E16M340), combined platinum and
157 Ag/AgCl (E31M004) electrode and EC conductivity cell (CDC 30T-3), respectively. Carbon content in
158 dry samples was determined by dry combustion (900°C, V₂O₅ for total carbon – TC; 200°C, 25 % H₃PO₄
159 for inorganic carbon – IC) and analysis of evolved CO₂ by means of TOC-VCSH with SSM-5000A
160 module (Shimadzu, Japan). Total organic carbon (TOC) was calculated from the difference of TC and
161 IC.

162 Concentrations of biogenic nitrogen and phosphorus were determined colourimetrically using
163 an automated, continuous-flow device AutoAnalyzer3 (Bran & Luebbe, Germany) as described in
164 details elsewhere (Stepniewska et al., 2013).

165 **2.3. BHP extraction and purification**

166 Sediment samples were extracted using a modified Bligh-Dyer method (Bischoff et al., 2016;
167 Doğrul Selver et al., 2015; Sparkes et al., 2015). Five grams of sediment was ultrasonically extracted
168 using a monophasic mixture of methanol/dichloromethane/de-ionised water (2:1:0.8 v/v/v). The
169 supernatant was separated by centrifugation and the remaining sediments re-extracted twice. Organic
170 phases were split into organic and aqueous phases by adding further DCM and water (final ratio 1:1:0.9
171 v/v/v). The combined organic phases were evaporated to dryness using a gentle nitrogen stream.

172 NH₂ solid phase extraction (SPE) cartridges (1 g/6 mL; Isolute, Biotage, Sweden) were pre-
173 conditioned with 6 mL hexane. Organic phases were then dissolved in 200 µL DCM and loaded onto
174 the cartridge, and separated into two fractions. Fraction one, containing non-polar and acidic, was
175 collected using 6 mL of diethyl ether/acetic acid [98:2, v:v]). Fraction two, containing polar compounds,
176 including BHPs, was collected using 12 mL methanol. After separation, the internal standard (5α-
177 pregnane-3β,20β-diol) was added to fraction two and dried under nitrogen. This SPE method was
178 adapted from a method commonly used in other studies of complex polar lipids from environmental
179 samples (e.g. Lupascu et al., 2014).

180 Fraction two was acetylated with pyridine/acetic anhydride (1:1, v:v; 500 µL) for 1 h at 50 °C
181 and left at room temperature overnight. The samples were evaporated to dryness, re-dissolved in

182 methanol/propan-2-ol (60:40, v:v) and filtered through a 0.2 μm PTFE syringe filter. For BHP analysis,
183 samples were dissolved in methanol/propan-2-ol (60:40, v:v; 500 μL). Sample injection volume was 10
184 μL .

185 **2.4. HPLC-Q-TOF-MS analyses**

186 BHPs were identified and measured using reverse phase high performance liquid
187 chromatography/atmospheric pressure chemical ionisation – mass spectrometry (HPLC/APCI-MS),
188 using a method adapted from Cooke et al. (2008). An Agilent 1200 series HPLC was coupled to an
189 Agilent Technologies 6540 UHD Accurate-Mass Q-TOF mass spectrometer equipped with a positive
190 ion APCI source. Separation was achieved using a 15cm C_{18} column and solvent gradients as follows.
191 Solvent A was a mixture of methanol and de-ionised water (90:10 v/v). Solvent B was a mixture of
192 methanol 2-propanol and water (59:40:1 v/v/v). Solvent gradients were initially 100% A, linear to 100%
193 B at 25 minutes, held for 15 min. Following BHP separation, the column was backflushed to remove
194 contaminants and equilibrated at 100% A. The conditions for APCI were drying gas (N_2) flow 8L/min
195 and temperature 300°C, nebuliser pressure 35psig, vaporiser temperature 400°C, capillary voltage
196 3.5kV and corona 8 μA .

197 BHP structures were identified based on previously published spectra, including comparison of
198 absolute and relative retention times, major ions and MS^2 ions (Cooke et al., 2008). Semi-quantitative
199 estimation of BHP concentration was achieved by comparing base peak ion areas of individual BHPs to
200 the m/z 345 chromatogram base peak area (acetylated 5 α -pregnane-3 β ,20 β -diol internal standard).
201 Relative response factors relative to the internal standard, determined from a suite of acetylated BHP
202 standards, were used to adjust the BHP peak areas (for further details see van Winden et al., 2012). Each
203 sample was injected in triplicate. The average reproducibility of triplicate injections was very good:
204 average 5% RSD ($\pm 0.23 \mu\text{g g}^{-1}$ sediment; 1 standard deviation) for BHT and 5% RSD ($\pm 0.01 \mu\text{g g}^{-1}$
205 sediment) for aminotriol.

206 **2.5. Statistical analyses**

207 Correlation coefficients between the studied variables were calculated with Pearson algorithm using
 208 Statistica 13 (Statsoft, USA). A graphical display of the correlation matrix was created using TBtools
 209 toolkit (Chen et al., 2020). Bray-Curtis similarity matrices representing the studied physical and
 210 chemical properties were analyzed using non-metric multidimensional scaling (NMDS) in PAST 4.03
 211 (Hammer et al., 2001). NMDS was used to detect patterns that could explain the observed similarities
 212 or dissimilarities among the samples

213 3. Results

214 3.1. Physical and chemical properties

215 The sediments studied differed significantly in terms of lithology, which affected their physico-
 216 chemical properties. Lignite samples were the most distinctive group. Their TOC content was generally
 217 >60% (except PGB-W1, TOC 39%). High TOC content was accompanied by high humidity. Lignite
 218 samples were generally characterized by near neutral pH. In the group of mineral sediments, there were
 219 significant differences in pH between samples derived from the PGT and PGB. PGT overburden samples
 220 were characterized by slightly alkaline (pH close to 8) while BD by acidic (pH 2 to 5) reaction. Samples
 221 differed also in terms of concentration of the pore solute. The EC values determined in PGB sediments
 222 were much higher than in the PGT ones. In all the samples studied nitrogen was mainly represented by
 223 N-NH₄. The distribution of the nitrogen biogenic forms and P-PO₄ was not dependent on location or
 224 lithology. The specific values concerning each of the studied parameters are presented in Table 2.

225 Tab. 2. Means and standard deviations (SD) of physical and chemical properties of the analysed
 226 samples.

Sample		PGT- ST2	PGT- ST1	PGT - W2	PGT- SP	PGT - W1	PGB- ST2	PGB- ST1	PGB - W1	PGB - W2	PGB- SP
Moisture	Mean	2.35	18.53	66.57	14.09	80.99	27.45	20.30	69.74	62.39	26.55
	SD	0.15	2.07	6.50	0.89	3.11	7.00	0.92	13.31	4.58	0.14
pH	Mean	8.10	7.94	6.25	7.95	7.71	2.04	5.42	6.83	5.94	5.27
	SD	0.08	0.01	0.03	0.01	0.03	0.01	0.01	0.01	0.02	0.02
EC	Mean	0.054	0.190	0.572	0.427	0.582	1.893	1.069	0.333	0.908	1.126
	SD	0.004	0.003	0.001	0.001	0.001	0.003	0.002	0.003	0.001	0.001
	Mean	4.71	2.98	0.41	0.53	0.94	1.81	4.73	4.68	1.54	2.47

N-NO ₃ mg kg ⁻¹	SD	5.07	2.15	0.13	0.50	0.86	1.02	2.00	0.87	1.98	1.38
N-NH ₄ mg kg ⁻¹	Mean	44.33	41.37	25.13	12.27	27.54	36.72	29.51	28.94	38.46	36.23
	SD	10.85	8.50	6.24	9.52	11.55	1.11	3.12	12.35	3.33	1.64
P-PO ₄ mg kg ⁻¹	Mean	1.32	41.38	9.39	21.07	2.64	0.80	1.44	0.58	19.41	1.14
	SD	0.39	12.91	6.33	4.76	1.19	0.50	0.26	0.73	12.77	0.43
IC %	Mean	<0.001	0.101	<0.001	0.360	<0.001	<0.001	0.008	<0.001	<0.001	<0.001
	SD	<0.001	0.016	<0.001	0.001	<0.001	<0.001	0.001	<0.001	<0.001	<0.001
TOC %	Mean	0.03	6.30	68.38	0.47	67.31	0.29	0.10	39.05	65.29	3.25
	SD	0.05	0.08	3.09	0.27	2.12	0.05	0.01	2.18	2.52	0.49

227

228 3.2. BHP analysis

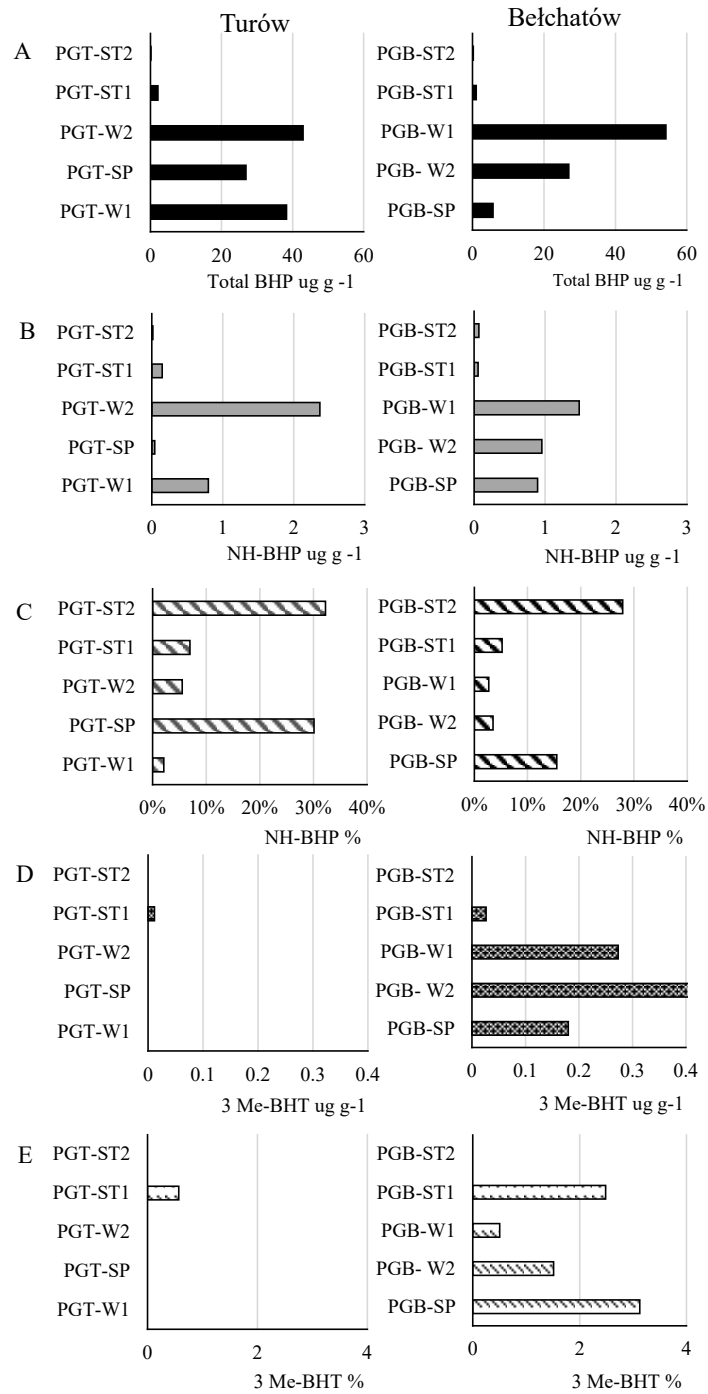
229 All samples contained measurable BHPs, although their concentrations varied by a factor of
 230 nearly 300 (Fig.2A). In general, lignites were richer in BHPs than the mineral samples. The highest
 231 concentration of BHPs was found in the PGB-W1 (54.13 µg g⁻¹). The concentration of BHPs in the other
 232 lignite from this location was 50 % lower. The concentration of BHPs in Turów lignites was less diverse
 233 (from 47 to 49 µg g⁻¹ in PGT-W1 and PGT-W2, respectively) but still several times higher than in the
 234 mineral samples. The lowest values of the total BHP concentration were determined for the PGT-ST2
 235 (2.2 µg g⁻¹) (Fig. 2A).

236 In general, the NH-BHP distribution followed the pattern described for the total BHPs (Fig. 2B).
 237 However, NH-BHPs made up a high proportion of the BHP composition of the mineral samples (Fig.
 238 2C).

239 Analysis of the NH-BHP speciation revealed that in majority of samples (except PGT-W2),
 240 aminotriol [1b] was predominant and present both as saturated and unsaturated compound. Aminotetrol
 241 [1c] was only found in one iso-form. Based on the aminotetrol/aminotriol ratio, it may be assumed that
 242 in all samples aminotetrol was of methanotrophic origin. In general, it was more abundant in lignites
 243 where it comprised up to 84% (PGT-W2) of the NH-BHPs (Fig. 3). In mineral samples aminotetrol was
 244 absent (PGT-ST1 and PGT-ST2) and/or was present at low concentration (Fig. 3). Distribution of
 245 aminopentol [1d] as the most diagnostic for methanotrophic bacteria depended on location. In the case
 246 of the Bełchatów deposit, aminopentol was present in all samples, while in Turów only in the mineral

247 overburden. The saturated form was found in mineral samples while unsaturated in lignites. The other
 248 methanotrophic biomarker, C-3 methylated aminotriol [2b] was found at low concentrations. It was
 249 absent in majority of the Turów samples (Fig. 2D-E).

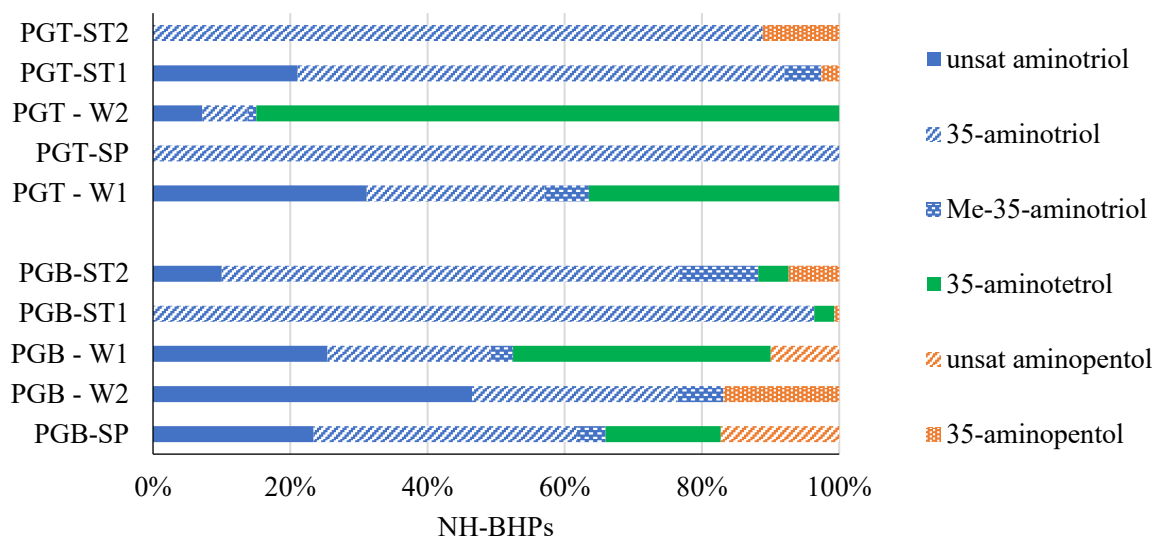
250



251

252 Fig. 2. Distribution of BHPs in the Turów and Bełchatów deposits. A - the amount of total BHPs, B -
 253 the amount of NH-BHPs, C- the share of NH-BHPs in the total BHPs pool, D – the amount of 3Me-
 254 BTH, E- the share of 3Me-BTH in the total BHPs pool.

255



256

257 Fig. 3. The average fractional abundance of NH-BHPs in lignites and mineral samples collected from
 258 the Turów and Bełchatów deposits.

259 4. Discussion

260 4.1. Distribution and speciation of BHPs

261 BHPs provide a record of the biological processes occurring in a given sediment. Using BHPs
 262 to trace microbiological processes in ancient sediments relies on understanding the environmental
 263 controls of their production (including the presence of modern microbial communities) and
 264 preservation (Osborne et al., 2017).

265 Generally, conditions found in the subsurface geological strata of lignite deposits are not suitable
 266 for aerobic micro-organisms (like MB). The most important limitation is restricted access to
 267 molecular oxygen. Traces of oxygen that are delivered with meteoric waters are rapidly utilized,
 268 mostly for the organic matter mineralization (Parnell and McMahon, 2016). However, Bełchatów
 269 and Turów lignite-bearing deposits are located at relatively shallow depths (Tab. 1). The overlying
 270 formations are characterized by high permeability (e.g. sands) and comprise a potential
 271 transportation route of the aerated meteoric waters (Jagóra and Szwed-Lorenz, 2005; Kasiński et al.,

272 2010). The deposits also remain in hydrological continuum with the surrounding water-bearing
273 strata (Szczepiński, 2018). The groundwater and nutrients may be thus delivered to sustain the
274 microbes, and the waterborne communities may penetrate the coal beds. Also anthropogenic, large-
275 scale hydrotechnical works related with exploitation of the deposits may contribute to enhanced
276 transportation of the aerated waters (Szczepiński, 2018) with potential to support growth of the MB.
277 Oxidation-reduction potentials measured in Turów and Bełchatów lignites were in the range
278 characteristic for suboxic or moderately reduced environments (Pytlak et al., 2020).

279 Nevertheless, the methanotrophic bacteria are characterized by vast array of metabolic
280 adaptations that enable long-term survival under extreme environmental conditions including not
281 only anoxia but also osmotic stress and/or high temperature (Sharp et al., 2014; Stępniewska et al.,
282 2018b). The presence of the MB in coal and the associated waters was already confirmed in many
283 deposits worldwide (Ivanov et al., 1979; Mills et al., 2010; Pytlak et al., 2020, 2014, Stępniewska
284 et al., 2014, 2013; Wolińska et al., 2013). For this reason, it cannot be ruled out that some of the
285 BHPs are derived from the viable methanotrophs.

286 NH-BHP distribution in the lignite-bearing sequence (both Turów and Bełchatów deposits), shows
287 several times higher concentration of the methanotroph-specific compounds in lignites than in the
288 mineral overburden. This indicates the occurrence of the intrinsic methane turnover in the original
289 wetland and putatively also later. Similarly, in contemporary peat-forming ecosystems, high activity of
290 these microorganisms is noted and assumed to restrain majority of the CH₄ emissions (Stępniewska et
291 al., 2018a). As shown by other studies, in peatlands, aminopentol-producing type I MB are found mainly
292 in the uppermost, well aerated parts of the soil, while the deeper sections of the profile are dominated
293 by the type II MB (Esson et al., 2016; Rey-Sanchez et al., 2019) that contain only aminotetrol [1c] and
294 aminotriol [1b] compounds (Rush et al., 2016). In the studied lignites, the major NH-BHP compounds
295 were aminotriol and aminotetrol, with minor participation of aminopentol [1d] (Fig. 3). This feature
296 confirms that the methanotrophic community of the studied sediments was a combination of both type
297 I and type II methanotrophs, with the leading role of the latter. Bearing in mind ecophysiology of the
298 type I methanotrophs, and the present-day limited oxygen access to the studied strata, it is supposed that

299 aminopentol is most likely a remnant of the original wetland and indicates that the sediments developed
300 in at least partly aerated environments; Bełchatów lignites are described as detritic, detroxylic and
301 xylo-detritic (Szafranek-Nakonieczna et al., 2018). Development of such lithotypes is associated with
302 mires, forest swamps or moors (Widera, 2016a). Such ecosystems are not only characterized by
303 stratification of the oxidation-reduction conditions of the soil (Szafranek-Nakonieczna and Stępniewska,
304 2015), but also are occupied by a range of plants that live in association with the MB. Methanotrophic
305 endophytes affiliated to *Gammaproteobacteria* (type I, aminopentol-producing) were found in the
306 hyaline cells of the Sphagnum mosses (Raghoebarsing et al., 2005; Stępniewska et al., 2013) as well as
307 in the tissues of some wetland vascular plants (Stępniewska et al., 2018a). Recently, 25 % of microbial
308 communities residing within the tree bark were found to comprise type I MB.

309 Lignites derived from the Turów deposit did not contain aminopentol [1d]. It was only present in
310 the uppermost parts of the coal overburden. Such distribution is surprising, bearing in mind that the
311 compound was ubiquitously found in Bełchatów samples. Furthermore, Bełchatów and Turów lignites
312 represent similar lithotypes (Szafranek-Nakonieczna et al., 2018; Widera, 2016a). The lack of
313 aminopentol may be thus a result of specific diagenetic conditions that took place in the Turów basin.
314 In the Turów area, volcanic activity occurred during and probably after the formation of brown coal. It
315 is evidenced by basaltic intrusions located between the Neogene granitic basement of the basin and its
316 organic-rich sediment fill (Liber-Makowska, 2013). Confirmation of the influence of different
317 temperature-driven transformation of the organic matter in the two studied deposits (based on FTIR
318 assay of condensation of aromatic rings) was already presented in (Pytlak et al., 2020). Even today, the
319 amount of geothermal energy reaching the surface in the Turów area is much higher than in the
320 Bełchatów area (Majorowicz and Grad, 2020). Temperature is one of the most important factors
321 influencing the coalification (Strapoć et al., 2007) and the durability of biomarkers (Goryl et al., 2018).
322 It seems, therefore, that despite the fact that in living cells the concentration of aminopentol increases
323 with temperature (up to 40°C) (Osborne et al., 2017), in the long-term perspective of diagenetic
324 processes, the increased temperature causes the compound to break down. Similarly, the elevated
325 temperature might have been responsible for disappearance of 3-Me BHT [2a], which (with exception

326 of the PGT-ST1) was absent in Turów samples (Fig.2). Another evidence indicating the existence of
327 differences in the temperature of the studied deposits is the share of unsaturated compounds. Recently,
328 Bale et al. (2019) have shown that the proportion of unsaturated hopanols increases in methanotrophic
329 bacteria under low temperature conditions. Indeed, in the sediments obtained from the geothermally
330 heated Turów deposit, the share of unsaturated NH-BHPs was several times lower than in the sediments
331 from Bełchatów (Fig. 3).

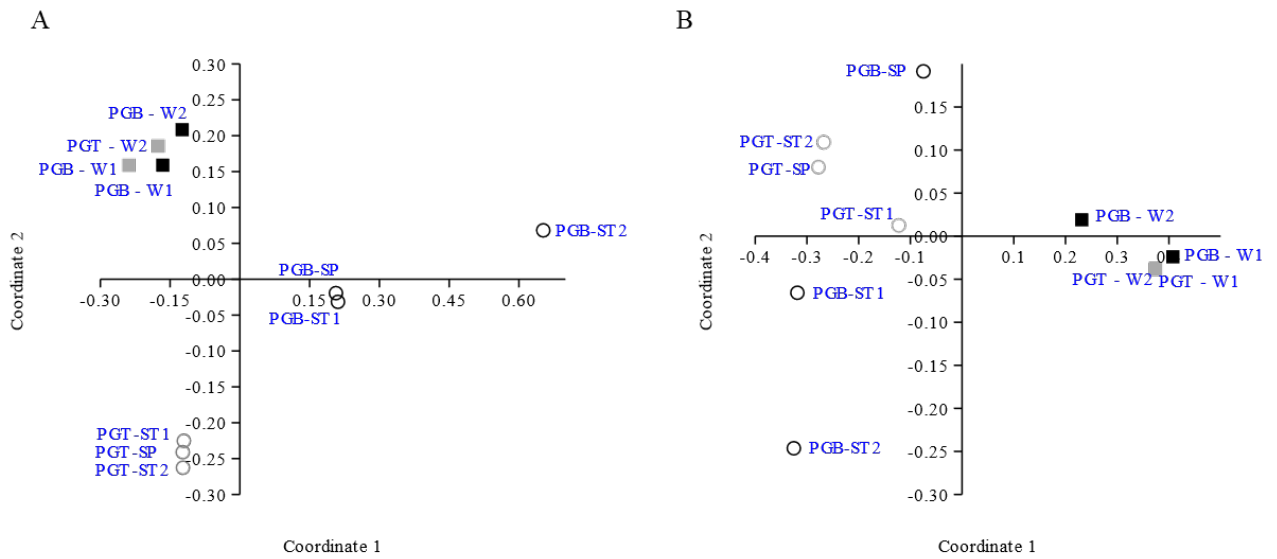
332 As already mentioned, the speciation of the NH-BHPs indicates the leading role of the type II MB
333 in oxidation of methane produced during coal diagenesis. These bacteria are known to be well adapted
334 to low oxygen (Walkiewicz and Brzezińska, 2019). Therefore, the burial of plant remnants might not
335 cause aerobic (microaerobic) methanotrophic activity to cease. . Over the years, new indications have
336 emerged that the obligatory methanotrophy paradigm is not true, especially in type II MB. It has been
337 demonstrated that some type II MB are capable of retaining viability by fermentation of endogenous
338 substrates (Vecherskaya et al., 2009). Also fermentation of exogenous substrates was suggested to serve
339 as a basis of survival of these aerobic bacteria under anaerobic conditions, but mechanisms of these
340 processes remain unclear (Roslev and King, 1995). Recent discoveries revealed that some type II MB
341 are also capable of mixotrophic growth on H₂ and CH₄ (Hakobyan and Liesack, 2020). Metabolic
342 flexibility might be the key for success in the type II MB survival in the lignites explaining speciation
343 of the BHPs.

344 The transition of microorganisms into the state of cryptobiosis as a consequence of environmental
345 stress may also be one of the reasons for the significant share of aminotriol in the overall pool of NH-
346 BHPs. In the course of depositing subsequent layers of sediments, the communities of microorganisms
347 were exposed to increasing stress resulting from the decreasing availability of oxygen. Osborne et al.
348 (2017) showed that the amount of aminotriol (which is produced by both methanotrophs type I and II)
349 in the cell membranes increases in the late stationary phase and under starvation conditions.

350 **4.2. NH-BHPs of the mineral cover**

351 It should be noted that in mineral sediments, characterized by very low concentration of BHPs, NH-
352 BHPs structures accounted for a significant proportion of the total BHP pool (up to 32%). The high
353 share of BHP-NH confirms that the coal seams exerted a significant influence on the composition of the
354 microbiome of the surrounding geological formations. Even in the youngest of the studied samples
355 (PGB-ST2), representing glaciolacustrine grey sand layers, methanotrophy seems to be an important
356 metabolic strategy. NH-BHPs comprised more than 20 % of the total BHP pool found in this sample
357 (Fig. 2). Bearing in mind that the glacial deposits in the Bełchatów area are connected with the Middle-
358 Polish glaciations that ended tens of thousands of years ago (Marks, 2005), the high abundance of
359 methanotroph-specific biomarkers suggests that at the time, methane was still emitted from the
360 decomposing organic matter, although at smaller quantities than at the early stages of diagenesis. It
361 seems that Bełchatów and Turów lignite deposits may have an impact on the microbiota of overburden
362 deposits also today. The accumulated methane, was found both in the Bełchatów and Turów deposits
363 (Macuda et al., 2011). Moreover, studies performed by Szafranek-Nakonieczna et al. (2018) indicate
364 that in some parts of the Bełchatów deposit, small quantities of methane are still produced biologically.
365 It would be thus reasonable to identify the influence of these emissions on the methanotrophy of the
366 uppermost layers of the profile, also by biomarker studies. However, the soil cover above the deposits
367 is largely transformed by the anthropogenic activity or removed due to the mining operations.

368

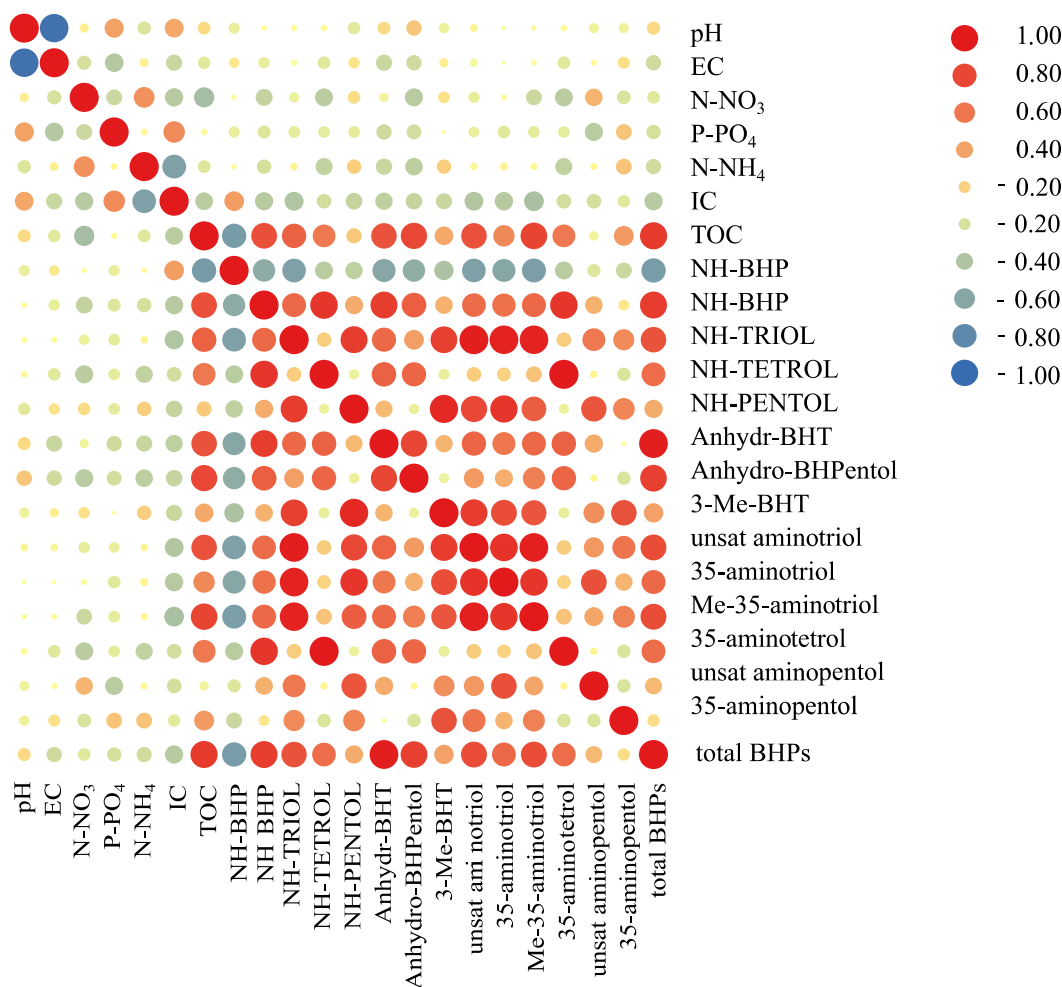


369

370 Fig. 4. Non-metric multidimensional scaling (NMDS) plot based on: A –biomarker record (stress
 371 0.0415), B – physical and chemical properties (stress 0.0407). Scaling was based on Bray–Curtis
 372 similarity distances.

373 NMDS ordination plots based on Bray-Curtis similarity indexes of the data comprising physico-
 374 chemical properties (Fig. 4A) and the composition of methanotrophic biomarkers (Fig. 4B) show that
 375 in both cases the coal samples were separated from the mineral samples. This confirms that in the organic
 376 matter–rich habitats, regardless of location, there is a system-specific composition of biomarkers,
 377 consisting of compounds derived from methanotrophs active in acrotelm (oxygenated part of the profile)
 378 and the catotelm (flooded part of the profile), as well as possibly at later stages of diagenesis. The organic
 379 matter content can be thus recognized as the main driving force shaping composition of the
 380 methanotrophic microbial community in the coalbed profile. Indeed, among the analyzed physical and
 381 chemical properties, only TOC correlated significantly with values characterizing the methanotroph-
 382 specific BHPs (Fig. 5).

383



384
 385 Fig. 5. Visualization of the correlation matrix of the physicochemical properties of the studied
 386 sediments and BHPs.

387 Research concerning methane cycling in ancient deposits is scarce, but extensive studies concerning
 388 some Palaeogene lignite layers of Cobham (UK; (Pancost et al., 2007) and Schöningen, (Germany;
 389 (Inglis et al., 2015) confirm that bacterially-derived biomarkers are preserved in coal-bearing series. The
 390 authors also suggested (based on $\delta^{13}\text{C}$ depletion of the isolated hopanes) the important role of the aerobic
 391 methanotrophic metabolism in the carbon turnover in the coal, which is similar to the results achieved
 392 for the Turów and Bełchatów deposits. Recently, Talbot et al. (2016) have described distribution of the
 393 methanotroph-specific polyfunctionalised hopanoids of the Cobham lignite occurring in the Cobham
 394 Lignite Sequence. The results from Cobham show many similarities with those presented herein. They
 395 are manifested, among others, in the proportions between NH-BHP forms. However, unlike in
 396 Bełchatów or Turów, in the Cobham profile, the amounts of methanotroph-specific NH-BHPs found in

397 the mineral samples were much higher than in the coal itself. The authors suggested that this may be
398 explained by better preservation of the biomarker compounds in the fine-grained sediment. Results
399 presented here are contrary: regardless of lithology, the mineral samples contained less BHPs.

400 **Conclusions**

401 Taking into account the data presented in earlier studies of BHP occurrence in lignites and the
402 present results, it may be assumed that content and speciation of BHPs depend on many circumstances
403 with the leading role of the living conditions of microorganisms (especially the availability of CH₄ and
404 O₂) and diagenesis (with a particular negative impact of increased temperature). The practical aspect of
405 the presented results given that lignites, composed of organic matter at a relatively early stage of
406 diagenesis, are the subject of intensive research aimed at determining the possibility of biological and
407 in situ gasification to methane. The obtained results show a strong relationship between MB and the
408 deposited organic matter. In the light of the literature data (e.g. Ivanov et al., 1979; Mills et al., 2010;
409 Pytlak et al., 2020, 2014; Stepniewska et al., 2014, 2013; Wolińska et al., 2013), it cannot be excluded
410 that part of the BHPs comes from the viable population of these microorganisms. As reports from other
411 ecosystems show, MB can be very effective in the utilization of methane (Mayr et al., 2020; Rogener et
412 al., 2018), which should be taken into account when planning the use of lignite deposits as a source of
413 this raw material.

414 **Contributor Roles**

415 Anna Pytlak: Conceptualization, Investigation, Formal analysis, Writing—, Methodology,
416 Visualization, Funding acquisition; Robert Sparkes: Investigation, Writing—; Saule Akmetkaliyeva:
417 investigation; Weronika Goraj: Investigation; Anna Szafranek-Nakonieczna: Investigation; Artur
418 Banach: Investigation; Mirosław Słowakiewicz: Writing, Resources.

419 **Acknowledgements**

420 The authors acknowledge PGE Górnictwo i Energetyka Konwencjonalna S.A. Oddziały
421 Kopalnia Węgla Brunatnego Bełchatów and Turów for allowing access to the coalbeds and providing
422 information about geology of the sampled areas.

423 **Funding**

424 The work was supported by the National Science Centre, Poland (2018/02/X/NZ9/01107 and
425 2015/17/B/NZ9/01662).

426 **References**

- 427 Arning, N., Wilson, D.J., 2020. The past, present and future of ancient bacterial DNA. *Microb.*
428 *Genomics* 6, 1–19. <https://doi.org/10.1099/mgen.0.000384>
- 429 Bale, N.J., Irene Rijpstra, W.C., Sahonero-Canavesi, D.X., Oshkin, I.Y., Belova, S.E., Dedysh, S.N.,
430 Sinninghe Damsté, J.S., 2019. Fatty acid and hopanoid adaption to cold in the methanotroph
431 *methylovulum psychrotolerans*. *Front. Microbiol.* 10, 1–13.
432 <https://doi.org/10.3389/fmicb.2019.00589>
- 433 Barkley, Z.R., Lauvaux, T., Davis, K.J., Deng, A., Fried, A., Weibring, P., Richter, D., Walega, J.G.,
434 DiGangi, J., Ehrman, S.H., Ren, X., Dickerson, R.R., 2019. Estimating Methane Emissions From
435 Underground Coal and Natural Gas Production in Southwestern Pennsylvania. *Geophys. Res.*
436 *Lett.* 46, 4531–4540. <https://doi.org/10.1029/2019GL082131>
- 437 Bidle, K.D., Lee, S.H., Marchant, D.R., Falkowski, P.G., 2007. Fossil genes and microbes in the oldest
438 ice on Earth. *Proc. Natl. Acad. Sci. U. S. A.* 104, 13455–13460.
439 <https://doi.org/10.1073/pnas.0702196104>
- 440 Bischoff, J., Sparkes, R.B., Selver, A.D., Spencer, R.G.M., Gustafsson, Ö., Semiletov, I.P., Dudarev,
441 O. V., Wagner, D., Rivkina, E., Van Dongen, B.E., Talbot, H.M., 2016. Source, transport and
442 fate of soil organic matter inferred from microbial biomarker lipids on the East Siberian Arctic
443 Shelf. *Biogeosciences* 13, 4899–4914. <https://doi.org/10.5194/bg-13-4899-2016>
- 444 Cai, P., Huang, Q.Y., Zhang, X.W., 2006. Interactions of DNA with clay minerals and soil colloidal
445 particles and protection against degradation by DNase. *Environ. Sci. Technol.* 40, 2971–2976.
446 <https://doi.org/10.1021/es0522985>
- 447 Cappellini, E., Prohaska, A., Racimo, F., Welker, F., Pedersen, M.W., Allentoft, M.E., De Barros
448 Damgaard, P., Gutenbrunner, P., Dunne, J., Hammann, S., Roffet-Salque, M., Ilardo, M.,
449 Moreno-Mayar, J.V., Wang, Y., Sikora, M., Vinner, L., Cox, J., Evershed, R.P., Willerslev, E.,

450 2018. Ancient Biomolecules and Evolutionary Inference. *Annu. Rev. Biochem.* 87, 1029–1060.
451 <https://doi.org/10.1146/annurev-biochem-062917-012002>

452 Chen, C., Chen, H., Zhang, Y., Thomas, H.R., Frank, M.H., He, Y., Xia, R., 2020. TBtools: An
453 Integrative Toolkit Developed for Interactive Analyses of Big Biological Data. *Mol. Plant* 13,
454 1194–1202. <https://doi.org/10.1016/j.molp.2020.06.009>

455 Chiri, E., Greening, C., Lappan, R., Waite, D.W., Jirapanjawan, T., Dong, X., Arndt, S.K., Nauer, P.A.,
456 2020. Termite mounds contain soil-derived methanotroph communities kinetically adapted to
457 elevated methane concentrations. *ISME J.* 14, 2715–2731. [https://doi.org/10.1038/s41396-020-](https://doi.org/10.1038/s41396-020-0722-3)
458 [0722-3](https://doi.org/10.1038/s41396-020-0722-3)

459 Cooke, M.P., Talbot, H.M., Wagner, T., 2008. Tracking soil organic carbon transport to continental
460 margin sediments using soil-specific hopanoid biomarkers: A case study from the Congo fan
461 (ODP site 1075). *Org. Geochem.* 39, 965–971.
462 <https://doi.org/10.1016/j.orggeochem.2008.03.009>

463 Dean, J.F., Middelburg, J.J., Röckmann, T., Aerts, R., Blauw, L.G., Egger, M., Jetten, M.S.M., de
464 Jong, A.E.E., Meisel, O.H., Rasigraf, O., Slomp, C.P., in't Zandt, M.H., Dolman, A.J., 2018.
465 Methane Feedbacks to the Global Climate System in a Warmer World. *Rev. Geophys.* 56, 207–
466 250. <https://doi.org/10.1002/2017RG000559>

467 Doğrul Selver, A., Sparkes, R.B., Bischoff, J., Talbot, H.M., Gustafsson, Ö., Semiletov, I.P., Dudarev,
468 O. V., Boulton, S., van Dongen, B.E., 2015. Distributions of bacterial and archaeal membrane
469 lipids in surface sediments reflect differences in input and loss of terrestrial organic carbon along
470 a cross-shelf Arctic transect. *Org. Geochem.* 83–84, 16–26.
471 <https://doi.org/10.1016/j.orggeochem.2015.01.005>

472 Edenhofer, O., Pichs-Madruga, R., Sokona, Y., Minx, J.C., Farahani, E., Kadner, S., Seyboth, K.,
473 2015. Climate change 2014. Mitigation of climate change. Summary for policymakers and
474 technical summary. Working Group III contribution to the fifth assessment report of the
475 Intergovernmental Panel on Climate Change (IPCC). *Annu. Rev. Environ. Resour.* 40, 363–394.
476 <https://doi.org/10.1146/annurev-environ-021113-095626>

477 Ellegaard, M., Clokie, M.R.J., Czymionka, T., Frisch, D., Godhe, A., Kremp, A., Letarov, A.,

478 McGenity, T.J., Ribeiro, S., John Anderson, N., 2020. Dead or alive: sediment DNA archives as
479 tools for tracking aquatic evolution and adaptation. *Commun. Biol.* 3, 1–11.
480 <https://doi.org/10.1038/s42003-020-0899-z>

481 Esson, K.C., Lin, X., Kumaresan, D., Chanton, J.P., Murrell, J.C., Kostka, J.E., 2016. Alpha-and
482 gammaproteobacterial methanotrophs codominate the active methane-oxidizing communities in
483 an acidic boreal peat bog. *Appl. Environ. Microbiol.* 82, 2363–2371.
484 <https://doi.org/10.1128/AEM.03640-15>

485 Goryl, M., Marynowski, L., Brocks, J.J., Bobrovskiy, I., Derkowski, A., 2018. Exceptional
486 preservation of hopanoid and steroid biomarkers in Ediacaran sedimentary rocks of the East
487 European Craton. *Precambrian Res.* 316, 38–47. <https://doi.org/10.1016/j.precamres.2018.07.026>

488 Graham, D.W., Chaudhary, J.A., Hanson, R.S., Arnold, R.G., 1993. Factors affecting competition
489 between type I and type II methanotrophs in two-organism, continuous-flow reactors. *Microb.*
490 *Ecol.* 25, 1–17. <https://doi.org/10.1007/BF00182126>

491 Hammer, Ø., Harper, D.A.T., Ryan, P.D., 2001. Past: Paleontological statistics software package for
492 education and data analysis. *Palaeontol. Electron.* 4, 1–9.

493 Inglis, G.N., Collinson, M.E., Riegel, W., Wilde, V., Robson, B.E., Lenz, O.K., Pancost, R.D., 2015.
494 Ecological and biogeochemical change in an early Paleogene peat-forming environment: Linking
495 biomarkers and palynology. *Palaeogeogr. Palaeoclimatol. Palaeoecol.* 438, 245–255.
496 <https://doi.org/10.1016/j.palaeo.2015.08.001>

497 Inglis, G.N., Naafs, B.D.A., Zheng, Y., Schellekens, J., Pancost, R.D., 2019. $\delta^{13}\text{C}$ values of bacterial
498 hopanoids and leaf waxes as tracers for methanotrophy in peatlands. *Geochim. Cosmochim. Acta*
499 260, 244–256. <https://doi.org/10.1016/j.gca.2019.06.030>

500 Ivanov, M. V., Beliaev, S.S., Laurinavichus, K.S., Namsaraev, B.B., 1979. Mikrobiologicheskoe
501 okislenie metaba v plastovykh vodakh Nizhnego Povolzh'ia. *Mikrobiologiya* 48, 129–132.

502 Jagóra, E., Szwed-Lorenz, J., 2005. Analysis of variability of the main parameters of the brown coal
503 deposit in the West part of the Szczerców field. *Pr. Nauk. Inst. Górnictwa Politech.*
504 *Wrocławskiej, Stud. i Mater.* 113, 50–51.

505 Jahnke, L.L., Summons, R.E., Hope, J.M., Des Marais, D.J., 1999. Carbon isotopic fractionation in

506 lipids from methanotrophic bacteria II: The effects of physiology and environmental parameters
507 on the biosynthesis and isotopic signatures of biomarkers. *Geochim. Cosmochim. Acta* 63, 79–
508 93. [https://doi.org/10.1016/S0016-7037\(98\)00270-1](https://doi.org/10.1016/S0016-7037(98)00270-1)

509 Kasiński, J.R., 1983. Mechanizmy sedymentacji cyklicznej osadów trzeciorzędowych w zapadliskach
510 przedpola Sudetów. *Przegląd Geol.* 31, 237–243.

511 Kasiński, J.R., Piwocki, M., Swadowska, E., Ziemińska-Tworzydło, M., 2010. Lignite of the polish
512 Lowlands miocene: Characteristics on a base of selected profiles. *Biul. - Państw. Inst. Geol.* 99–
513 154.

514 Kholod, N., Evans, M., Pilcher, R.C., Roshchanka, V., Ruiz, F., Coté, M., Collings, R., 2020. Global
515 methane emissions from coal mining to continue growing even with declining coal production. *J.*
516 *Clean. Prod.* 256, 120489. <https://doi.org/10.1016/j.jclepro.2020.120489>

517 Knief, C., 2015. Diversity and habitat preferences of cultivated and uncultivated aerobic
518 methanotrophic bacteria evaluated based on pmoA as molecular marker. *Front. Microbiol.* 6, 1–
519 38. <https://doi.org/10.3389/fmicb.2015.01346>

520 Kusch, S., Wakeham, S.G., Sepúlveda, J., 2021. Diverse origins of “soil marker”
521 bacteriohopanepolyols in marine oxygen deficient zones. *Org. Geochem.* 151, 104150.
522 <https://doi.org/10.1016/j.orggeochem.2020.104150>

523 Liber-Makowska, E., 2013. Geothermal conditions of the Turoszów Basin (in Polish). *Tech. Poszuk.*
524 *Geol. Geoterm. Zrównoważony Rozw.* 1, 135–142.

525 Lupascu, M., Welker, J.M., Seibt, U., Maseyk, K., Xu, X., Czimczik, C.I., 2014. High Arctic wetting
526 reduces permafrost carbon feedbacks to climate warming. *Nat. Clim. Chang.* 4, 51–55.
527 <https://doi.org/10.1038/nclimate2058>

528 Macuda, J., Nodzeński, A., Wagner, M., Zawisza, L., 2011. Sorption of methane on lignite from
529 Polish deposits. *Int. J. Coal Geol.* 87, 41–48. <https://doi.org/10.1016/j.coal.2011.04.010>

530 Majorowicz, J.A., Grad, M., 2020. Differences Between Recent Heat Flow Maps of Poland and Deep
531 Thermo-Seismic and Tectonic Age Constraints. *Int. J. Terr. Heat Flow Appl.* 3, 11–19.
532 <https://doi.org/10.31214/ijthfa.v3i1.45>

533 Marks, L., 2005. Pleistocene glacial limits in the territory of Poland. *Prz. Geol.* 53, 988–993.

534 Marshall, N.T., Vanderploeg, H.A., Chaganti, S.R., 2021. Environmental (e)RNA advances the
535 reliability of eDNA by predicting its age. *Sci. Rep.* 11, 2769. [https://doi.org/10.1038/s41598-](https://doi.org/10.1038/s41598-021-82205-4)
536 021-82205-4

537 Mastej, W., Bartus, T., Rydlewski, J., 2015. Analysis of lithofacies cyclicity in the Miocene Coal
538 Complex of the Bełchatów lignite deposit, south-central Poland. *Geologos* 21, 285–302.
539 <https://doi.org/10.1515/logos-2015-0021>

540 Mayr, M.J., Zimmermann, M., Dey, J., Brand, A., Wehrli, B., Bürgmann, H., 2020. Growth and rapid
541 succession of methanotrophs effectively limit methane release during lake overturn. *Commun.*
542 *Biol.* 3, 1–9. <https://doi.org/10.1038/s42003-020-0838-z>

543 Mills, C.T., Amano, Y., Slater, G.F., Dias, R.F., Iwatsuki, T., Mandernack, K.W., 2010. Microbial
544 carbon cycling in oligotrophic regional aquifers near the Tono Uranium Mine, Japan as inferred
545 from $\delta^{13}\text{C}$ and $\Delta^{14}\text{C}$ values of in situ phospholipid fatty acids and carbon sources. *Geochim.*
546 *Cosmochim. Acta* 74, 3785–3805. <https://doi.org/10.1016/j.gca.2010.03.016>

547 Myśkow, E., Krzyszkowski, D., Wachecka-Kotkowska, L., Wieczorek, D., 2016. Plant macrofossils
548 from the Czyżów Complex deposits of the Szczerców outcrop, central Poland. *Wydaw. AGH* 42,
549 325–336. <https://doi.org/10.7494/geol.2016.42.3.325>

550 Osborne, K.A., Gray, N.D., Sherry, A., Leary, P., Mejeha, O., Bischoff, J., Rush, D., Sidgwick, F.R.,
551 Birgel, D., Kalyuzhnaya, M.G., Talbot, H.M., 2017. Methanotroph-derived bacteriohopanepolyol
552 signatures as a function of temperature related growth, survival, cell death and preservation in the
553 geological record. *Environ. Microbiol. Rep.* 9, 492–500. [https://doi.org/10.1111/1758-](https://doi.org/10.1111/1758-2229.12570)
554 2229.12570

555 Pancost, R.D., Steart, D.S., Handley, L., Collinson, M.E., Hooker, J.J., Scott, A.C., Grassineau, N. V,
556 Glasspool, I.J., 2007. Increased terrestrial methane cycling at the Palaeocene–Eocene thermal
557 maximum. *Nature* 449, 332–335. <https://doi.org/https://doi.org/10.1038/nature06012>

558 Pandey, V.C., Singh, J.S., Singh, D.P., Singh, R.P., 2014. Methanotrophs: Promising bacteria for
559 environmental remediation. *Int. J. Environ. Sci. Technol.* [https://doi.org/10.1007/s13762-013-](https://doi.org/10.1007/s13762-013-0387-9)
560 0387-9

561 Pandit, P.S., Hoppert, M., Rahalkar, M.C., 2018. Description of ‘*Candidatus Methylocucumis oryzae*’,

562 a novel Type I methanotroph with large cells and pale pink colour, isolated from an Indian rice
563 field. *Antonie van Leeuwenhoek, Int. J. Gen. Mol. Microbiol.* 111, 2473–2484.
564 <https://doi.org/10.1007/s10482-018-1136-3>

565 Parnell, J., McMahon, S., 2016. Physical and chemical controls on habitats for life in the deep
566 subsurface beneath continents and ice. *Philos. Trans. R. Soc. A Math. Phys. Eng. Sci.* 374, 1–13.
567 <https://doi.org/10.1098/rsta.2014.0293>

568 Pawelec, S., Bielowicz, B., 2016. Petrographic composition of lignite from the Szczerców deposit,
569 Polish Lowlands. *Contemp. Trends Geosci.* 5, 92–103. <https://doi.org/10.1515/ctg-2016-0007>

570 Pedersen, M.W., Overballe-Petersen, S., Ermini, L., Der Sarkissian, C., Haile, J., Hellstrom, M.,
571 Spens, J., Thomsen, P.F., Bohmann, K., Cappellini, E., Schnell, I.B., Wales, N.A., Carøe, C.,
572 Campos, P.F., Schmidt, A.M.Z., Gilbert, M.T.P., Hansen, A.J., Orlando, L., Willerslev, E., 2015.
573 Ancient and modern environmental DNA. *Philos. Trans. R. Soc. B Biol. Sci.* 370, 1–11.
574 <https://doi.org/10.1098/rstb.2013.0383>

575 Pytlak, A., Stepniewska, Z., Kuźniar, A., Szafranek-Nakonieczna, A., Wolińska, A., Banach, A., 2014.
576 Potential for aerobic methane oxidation in Carboniferous coal measures. *Geomicrobiol. J.* 31,
577 737–747. <https://doi.org/10.1080/01490451.2014.889783>

578 Pytlak, A., Sujak, A., Szafranek-Nakonieczna, A., Grządziel, J., Banach, A., Goraj, W., Gałązka, A.,
579 Gruszecki, W.I., Stepniewska, Z., 2020. Water-induced molecular changes of hard coals and
580 lignites. *Int. J. Coal Geol.* 224, 103481. <https://doi.org/10.1016/j.coal.2020.103481>

581 Raghoebarsing, A.A., Smolders, A.J.P., Schmid, M.C., Rijpstra, W.I.C., Wolters-Arts, M., Derksen, J.,
582 Jetten, M.S.M., Schouten, S., Damsté, J.S.S., Lamers, L.P.M., Roelofs, J.G.M., Op Den Camp,
583 H.J.M., Strous, M., 2005. Methanotrophic symbionts provide carbon for photosynthesis in peat
584 bogs. *Nature* 436, 1153–1156. <https://doi.org/10.1038/nature03802>

585 Ratajczak, T., Hycnar, E., 2017. *Kopaliny towarzyszące w złożach węgla brunatnego. Geologiczno-*
586 *surowcowe aspekty zagospodarowania kopaliny towarzyszących.* Kraków.

587 Rey-Sanchez, C., Bohrer, G., Slater, J., Li, Y.-F., Grau-Andrés, R., Hao, Y., Rich, V.I., Davies, G.M.,
588 2019. The ratio of methanogens to methanotrophs and water-level dynamics drive methane
589 transfer velocity in a temperate kettle-hole peat bog. *Biogeosciences* 16, 3207–3231.

590 <https://doi.org/10.5194/bg-16-3207-2019>

591 Rogener, M.K., Bracco, A., Hunter, K.S., Saxton, M.A., Joye, S.B., 2018. Long-term impact of the
592 Deepwater Horizon oil well blowout on methane oxidation dynamics in the northern Gulf of
593 Mexico. *Elem Sci Anth* 6, 73. <https://doi.org/10.1525/elementa.332>

594 Roslev, P., King, G.M., 1995. Aerobic and anaerobic starvation metabolism in methanotrophic
595 bacteria. *Appl. Environ. Microbiol.* 61, 1563–1570. [https://doi.org/10.1128/aem.61.4.1563-](https://doi.org/10.1128/aem.61.4.1563-1570.1995)
596 [1570.1995](https://doi.org/10.1128/aem.61.4.1563-1570.1995)

597 Rush, D., Osborne, K.A., Birgel, D., Kappler, A., Hirayama, H., Peckmann, J., Poulton, S.W., Nickel,
598 J.C., Mangelsdorf, K., Kalyuzhnaya, M., Sidgwick, F.R., Talbot, H.M., 2016. The
599 Bacteriohopanepolyol Inventory of Novel Aerobic Methane Oxidising Bacteria Reveals New
600 Biomarker Signatures of Aerobic Methanotrophy in Marine Systems. *PLoS One* 11, e0165635.
601 <https://doi.org/10.1371/journal.pone.0165635>

602 Rush, D., Talbot, H.M., Van Der Meer, M.T.J., Hopmans, E.C., Douglas, B., Damsté, J.S.S., 2019.
603 Biomarker evidence for the occurrence of anaerobic ammonium oxidation in the eastern
604 Mediterranean Sea during Quaternary and Pliocene sapropel formation. *Biogeosciences* 16,
605 2467–2479. <https://doi.org/10.5194/bg-16-2467-2019>

606 Sharp, C.E., Smirnova, A. V., Graham, J.M., Stott, M.B., Khadka, R., Moore, T.R., Grasby, S.E.,
607 Strack, M., Dunfield, P.F., 2014. Distribution and diversity of Verrucomicrobia methanotrophs in
608 geothermal and acidic environments. *Environ. Microbiol.* 16, 1867–1878.
609 <https://doi.org/10.1111/1462-2920.12454>

610 Sinninghe Damsté, J.S., Rijpstra, W.I.C., Dedysh, S.N., Foesel, B.U., Villanueva, L., 2017. Pheno-
611 and genotyping of hopanoid production in Acidobacteria. *Front. Microbiol.* 8, 1–20.
612 <https://doi.org/10.3389/fmicb.2017.00968>

613 Sparkes, R.B., Doñrul Selver, A., Bischoff, J., Talbot, H.M., Gustafsson, Semiletov, I.P., Dudarev, O.
614 V., Van Dongen, B.E., 2015. GDGT distributions on the East Siberian Arctic Shelf: Implications
615 for organic carbon export, burial and degradation. *Biogeosciences* 12, 3753–3768.
616 <https://doi.org/10.5194/bg-12-3753-2015>

617 Stępniewska, Z., Goraj, W., Kuźniar, A., Szafranek-Nakonieczna, A., Banach, A., Górski, A., Pytlak,

618 A., Urban, D., 2018a. Methane Oxidation by Endophytic Bacteria Inhabiting Sphagnum sp. and
619 Some Vascular Plants. *Wetlands* 38, 411–422. <https://doi.org/10.1007/s13157-017-0984-3>

620 Stępniewska, Z., Goraj, W., Wolińska, A., Szafranek-Nakonieczna, A., Banach, A., Górski, A.,
621 Stępniewska, Z., Goraj, W., Wolinska, A., Szafranek-Nakonieczna, A., Banach, A., Gorski, A.,
622 2018b. Methanotrophic activity of rocks surrounding Badenian salts in the “Wieliczka” Salt
623 Mine. *Carpathian J. Earth Environ. Sci.* 13, 107 – 119.
624 <https://doi.org/10.26471/cjees/2018/013/011>

625 Stępniewska, Z., Kuźniar, A., Pytlak, A., Szymczycha, J., 2013. Detection of methanotrophic
626 endosymbionts in Sphagnum sp. originating from Moszne peat bog (East Poland). *African J.*
627 *Microbiol. Res.* 7, 1319–1325. <https://doi.org/10.5897/ajmr12.915>

628 Stępniewska, Z., Pytlak, A., Kuźniar, A., 2014. Distribution of the methanotrophic bacteria in the
629 Western part of the Upper Silesian Coal Basin (Borynia-Zofiówka and Budryk coal mines). *Int.*
630 *J. Coal Geol.* 130, 70–78. <https://doi.org/10.1016/j.coal.2014.05.003>

631 Stępniewska, Z., Pytlak, A., Kuźniar, A., 2013. Methanotrophic activity in Carboniferous coalbed
632 rocks. *Int. J. Coal Geol.* 106, 1–10. <https://doi.org/10.1016/j.coal.2013.01.003>

633 Szafranek-Nakonieczna, A., Stępniewska, Z., 2015. The influence of the aeration status (ODR, Eh) of
634 peat soils on their ability to produce methane. *Wetl. Ecol. Manag.* 23, 665–676.
635 <https://doi.org/10.1007/s11273-015-9410-x>

636 Szafranek-Nakonieczna, A., Zheng, Y., Słowakiewicz, M., Pytlak, A., Polakowski, C., Kubaczyński,
637 A., Bieganowski, A., Banach, A., Wolińska, A., Stępniewska, Z., 2018. Methanogenic potential
638 of lignites in Poland. *Int. J. Coal Geol.* 196, 201–210. <https://doi.org/10.1016/j.coal.2018.07.010>

639 Szczepiński, J., 2018. UWARUNKOWANIA HYDROGEOLOGICZNE WYDOBYCIA KOPALIN
640 W KOPALNIACH ODKRYWKOWYCH WĘGLA BRUNATNEGO HYDROGEOLOGICAL
641 CONDITIONS OF MINERAL RESOURCES EXTRACTION IN OPEN PIT MINES.
642 *Górnictwo Odkryw.* 59, 22–26.

643 Talbot, H.M., Bischoff, J., Inglis, G.N., Collinson, M.E., Pancost, R.D., 2016. Polyfunctionalised bio-
644 and geohopanoids in the Eocene Cobham Lignite. *Org. Geochem.* 96, 77–92.
645 <https://doi.org/10.1016/j.orggeochem.2016.03.006>

646 Talbot, H.M., Handley, L., Spencer-Jones, C.L., Bienvenu, D.J., Schefuß, E., Mann, P.J., Poulsen,
647 J.R., Spencer, R.G.M., Wabakanhanzi, J.N., Wagner, T., 2014. Variability in aerobic methane
648 oxidation over the past 1.2Myrs recorded in microbial biomarker signatures from Congo fan
649 sediments. *Geochim. Cosmochim. Acta* 133, 387–401. <https://doi.org/10.1016/j.gca.2014.02.035>

650 Thielemann, T., Lücke, A., Schleser, G.H., Littke, R., 2000. Methane exchange between coal-bearing
651 basins and the atmosphere: The Ruhr Basin and the Lower Rhine Embayment, Germany. *Org.*
652 *Geochem.* 31, 1387–1408. [https://doi.org/10.1016/S0146-6380\(00\)00104-2](https://doi.org/10.1016/S0146-6380(00)00104-2)

653 van Winden, J.F., Talbot, H.M., Kip, N., Reichart, G.J., Pol, A., McNamara, N.P., Jetten, M.S.M., Op
654 den Camp, H.J.M., Sinninghe Damsté, J.S., 2012. Bacteriohopanepolyol signatures as markers
655 for methanotrophic bacteria in peat moss. *Geochim. Cosmochim. Acta* 77, 52–61.
656 <https://doi.org/10.1016/j.gca.2011.10.026>

657 Vecherskaya, M., Dijkema, C., Saad, H.R., Stams, A.J.M., 2009. Microaerobic and anaerobic
658 metabolism of a *Methylocystis parvus* strain isolated from a denitrifying bioreactor. *Environ.*
659 *Microbiol. Rep.* 1, 442–449. <https://doi.org/10.1111/j.1758-2229.2009.00069.x>

660 Walkiewicz, A., Brzezińska, M., 2019. Interactive effects of nitrate and oxygen on methane oxidation
661 in three different soils. *Soil Biol. Biochem.* 133, 116–118.
662 <https://doi.org/10.1016/j.soilbio.2019.03.001>

663 Walkiewicz, A., Brzezińska, M., Wnuk, E., Jabłoński, B., 2020. Soil properties and not high CO₂
664 affect CH₄ production and uptake in periodically waterlogged arable soils. *J. Soils Sediments* 20,
665 1231–1240. <https://doi.org/10.1007/s11368-019-02525-x>

666 Walkiewicz, A., Bulak, P., Brzezińska, M., Włodarczyk, T., Polakowski, C., 2012. Kinetics of
667 methane oxidation in selected mineral soils. *Int. Agrophysics* 26, 401–406.
668 <https://doi.org/10.2478/v10247-012-0056-0>

669 Welander, P. V., Summons, R.E., 2012. Discovery, taxonomic distribution, and phenotypic
670 characterization of a gene required for 3-methylhopanoid production. *Proc. Natl. Acad. Sci. U. S.*
671 *A.* 109, 12905–12910. <https://doi.org/10.1073/pnas.1208255109>

672 Widera, M., 2016a. An overview of lithotype associations of Miocene lignite seams exploited in
673 Poland. *Geologos* 22, 213–225. <https://doi.org/10.1515/logos-2016-0022>

674 Widera, M., 2016b. Characteristics and origin of deformation structures within lignite seams – A case
675 study from polish opencast mines. *Geol. Q.* 60, 179–189. <https://doi.org/10.7306/gq.1268>

676 Widera, M., 2013. Changes of the lignite seam architecture - A case study from Polish lignite deposits.
677 *Int. J. Coal Geol.* 114, 60–73. <https://doi.org/10.1016/j.coal.2013.02.004>

678 Włodarczyk, T., Stepniewska, Z., Brzezińska, M., Pindelska, E., Przywara, G., 2004. Influence of
679 methane concentration on methanotrophic activity of Mollic Gleysol and Haplic Podzol. *Int.*
680 *Agrophysics* 18, 375–379.

681 Wolińska, A., Pytlak, A., Stepniewska, Z., Kuźniar, A., Piasecki, C., 2013. Identification of
682 methanotrophic bacteria community in the Jastrzebie-Moszczenica coal mine by fluorescence in
683 situ hybridization and PCR techniques. *Polish J. Environ. Stud.* 22, 275–282.

684 Zundel, M., Rohmer, M., 1985. Prokaryotic triterpenoids: 1. 3 β -Methylhopanoids from *Acetobacter*
685 species and *Methylococcus capsulatus*. *Eur. J. Biochem.* 150, 23–27.
686 <https://doi.org/10.1111/j.1432-1033.1985.tb08980.x>

687